



Published in final edited form as:

Cancer Res. 2009 October 1; 69(19): 7844–7850. doi:10.1158/0008-5472.CAN-09-1833.

Haplotype and Cell Proliferation Analyses of Candidate Lung Cancer Susceptibility Genes on Chromosome 15q24-25.1

Yan Liu¹, Pengyuan Liu¹, Weidong Wen¹, Michael A. James¹, Yian Wang¹, Joan E. Bailey-Wilson², Christopher I. Amos³, Susan M. Pinney⁴, Ping Yang⁵, Mariza de Andrade⁵, Gloria M. Petersen⁵, Jonathan S. Wiest⁶, Pamela R. Fain⁷, Ann G. Schwartz⁸, Adi Gazdar⁹, Colette Gaba¹⁰, Henry Rothschild¹¹, Diptasri Mandal¹¹, Elena Kupert⁴, Juwon Lee⁴, Daniela Seminara⁶, John Minna⁹, Marshall W. Anderson⁴, and Ming You¹

¹Washington University, St. Louis, Missouri ²National Human Genome Research Institute, Bethesda, Maryland ³M.D. Anderson Cancer Center, Houston, Texas ⁴University of Cincinnati, Cincinnati, Ohio ⁵Mayo Clinic College of Medicine, Rochester, Minnesota ⁶National Cancer Institute, Rockville, Maryland ⁷University of Colorado, Denver, Colorado ⁸Karmanos Cancer Institute, Detroit, Michigan ⁹University of Texas Southwestern Medical Center, Dallas, Texas ¹⁰University of Toledo College of Medicine, Toledo, Ohio ¹¹Louisiana State University Health Science Center, New Orleans, Louisiana

Abstract

Recent genome-wide association studies have linked the chromosome 15q24-25.1 locus to nicotine addiction and lung cancer susceptibility. To refine the 15q24-25.1 locus, we performed a haplotype-based association analysis of 194 familial lung cases and 219 cancer-free controls from the Genetic Epidemiology of Lung Cancer Consortium (GELCC) collection, and used proliferation and apoptosis analyses to determine which gene(s) in the 15q24-25.1 locus mediates effects on lung cancer cell growth *in vitro*. We identified two distinct subregions, *hapL* ($P = 3.20 \times 10^{-6}$) and *hapN* ($P = 1.51 \times 10^{-6}$), which were significantly associated with familial lung cancer. *hapL* encompasses *IREB2*, *LOC123688*, and *PSMA4*, and *hapN* encompasses the three nicotinic acetylcholine receptor subunit genes *CHRNA5*, *CHRNA3*, and *CHRNA4*. Examination of the genes around *hapL* revealed that *PSMA4* plays a role in promoting cancer cell proliferation. *PSMA4* mRNA levels were increased in lung tumors compared with normal lung tissues. Down-regulation of *PSMA4* expression decreased proteasome activity and induced apoptosis. Proteasome dysfunction leads to many diseases including cancer, and drugs that inhibit proteasome activity show promise as a form of cancer treatment. Genes around *hapN* were also investigated, but did not show any direct effect on lung cancer cell proliferation. We concluded that *PSMA4* is a strong candidate mediator of lung cancer cell growth, and may directly affect lung cancer susceptibility through its modulation of cell proliferation and apoptosis.

© 2009 American Association for Cancer Research.

Requests for reprints: Ming You, Department of Surgery and The Alvin J. Siteman Cancer Center, Washington University School of Medicine, 660 Euclid Avenue, Box 8109, St. Louis, MO. Phone: 314-362-9294; Fax: 314-362-9366; youm@wustl.edu. Y. Liu and P. Liu contributed equally to this work.

Note: Supplementary data for this article are available at Cancer Research Online (<http://cancerres.aacrjournals.org/>).

Disclosure of Potential Conflicts of Interest

No potential conflicts of interest were disclosed.

Introduction

Lung cancer is the leading cause of cancer death in both men and women worldwide (1). Many factors contribute to the risk of lung cancer including tobacco smoke and genetic variations among populations. Tobacco smoke is well established as the major risk factor for lung cancer; however, only 10% to 15% of long-term smokers develop lung cancer in their lifetime, suggesting a genetic predisposition to the disease (2). Benzo[a]pyrene and 4-(methylnitrosamino)-1-(3-pyridyl)-1-butanone in tobacco smoke are two major carcinogens that cause DNA damage, oxidative stress, and inflammation, thus promoting the initiation and growth of lung tumors (3,4). Nicotine in tobacco smoke is noncarcinogenic but highly addictive and acts through nicotinic acetylcholine receptors (nAChR). nAChRs are plasma membrane ion channels present in many tissues including the central and peripheral nervous systems and bronchial epithelial cells (5–8).

Both lung cancer and nicotine dependence studies have independently identified associations with the same variants of the 15q24-25.1 locus (9–12). Several highly significant single nucleotide polymorphisms (SNP) were identified in this locus, which spans a linkage disequilibrium block of ~240 kilobases and contains the genes *IREB2*, *LOC123688*, *PSMA4*, *CHRNA5*, *CHRNA3*, and *CHRNA4*. The *CHRN* genes encode for subunits of the nAChRs and were initially attractive candidates. Of the other genes in the locus, *IREB2* encodes an iron regulatory protein 2 and plays a central role in maintaining cellular iron homeostasis (13), *PSMA4* encodes a structural protein of the 20S proteasome core (14,15), and *LOC123688* is a hypothetical gene. It remains unclear whether the 15q24-25.1 locus has any direct or indirect effect on lung cancer susceptibility since many SNPs in this locus have high linkage disequilibrium. In the first scenario, a gene(s) in the 15q24-25.1 locus may regulate cell proliferation and/or apoptosis in the lung and thus predispose smokers to lung cancer. In the second scenario, polymorphisms in the locus may affect nicotine dependence and propensity to smoke, and thus increase the likelihood of developing lung cancer.

Based on our fine mapping analysis, we have systematically examined all of the six genes located in the 15q24-25.1 region for their role in regulating lung cancer cell growth *in vitro*. Via gene knockdown and apoptosis analyses, we showed that *PSMA4* at the 15q24-25.1 locus has a role in modulating human lung cancer cell proliferation. We further showed that *PSMA4* is required for proteasomal activities. Expression of *PSMA4* was increased in lung tumors compared with matched normal lung tissues. Our results suggest that *PSMA4* is a novel candidate gene that may contribute to lung cancer susceptibility.

Materials and Methods

Plasmids

Full-length cDNAs in cloning vectors encoding *IREB2* (BC017880), *LOC123688* (BC132753), *PSMA4* (BC047667), *CHRNA3* (BC001642), *CHRNA5* (BC033639), and *CHRNA4* (BC096080) were purchased from Open Biosystems, amplified by PCR, and subcloned into the *BamH I* and *Xho I* sites of pLenti6/V5-D-TOPO (pLV) vector (Invitrogen) to generate pLV-*IREB2*, pLV-*LOC123688*, pLV-*PSMA4*, pLV-*CHRNA5*, pLV-*CHRNA3*, and pLV-*CHRNA4*, respectively. PCR segments were confirmed by sequencing. Short hairpin RNAs in pLKO.1 lentiviral vectors for *IREB2*, *LOC123688*, *PSMA4*, and *CHRNA5* knockdown were purchased from Open Biosystems.

Cell lines

Human non-small cell lung cancer (NSCLC) cell lines A549 and H1299 were maintained in RPMI1640 supplemented with 10% fetal bovine serum (FBS) and 2 mmol/L glutamine.

293T cells were maintained in DMEM plus 10% FBS. The human nontumorigenic bronchial epithelial cell line HBEC3KT was maintained in keratinocyte serum-free medium (with 50 Ag/mL bovine pituitary extract and 5 ng/mL epidermal growth factor; Invitrogen). All cells were grown at 37°C in a humidified incubator with 5% CO₂.

Transfection, vira I packaging, and target cell infection

All transfections were performed using Lipofectamine 2000 (Invitrogen). To package lentiviral vectors, 293T cells were transfected with pLV or pLKO.1 vector along with pDMD Z6 and pΔ8.2. Thirty-six hours after transfection, the supernatant was harvested and spun at 3,000 rpm for 10 min at 4°C, and then incubated with target cells in the presence of 8 μg/mL polybrene (Sigma) for 24 h. Three days after infection, A549 cells were selected under 9 μg/mL blasticidin (Invitrogen) for 2 wk (for pLV positive cells) or 1 μg/mL puromycin (Sigma) for 3 d (for pLKO.1-positive cells), H1299 cells were selected under 6 μg/mL blasticidin for 2 wk or 1 μg/mL puromycin for 3 d, and HBEC3KT cells were selected under 6 μg/mL blasticidin for 2 wk. Antibiotic-resistant cells were pooled and expanded for further analysis under selective conditions.

Cell proliferation assay

Cells were seeded in a 96-well plate at 1,000 cells per well (100 μL aliquots) and cultured for a period of up to 4 d for A549 and 6 d for H1299. Viable cells were determined daily by MTT assay using the CellTiter 96 AQueous One Solution Cell Proliferation Assay kit (Promega) according to the manufacturer's instructions. All assays were performed to measure proliferation in triplicate wells.

RNA extraction, reverse transcription, and RT-quantitative PCR

Total RNAs of paired normal lung and lung tumor tissues were obtained from the Tissue Procurement Core at WUSTL. Total RNAs of cultured cells were extracted using Trizol (Invitrogen). To generate cDNA, 1 μg of total RNA was reverse transcribed (RT) using ImProm-II RT system (Promega). Twenty-five nanograms of the cDNA was used in a 25 μL total volume reaction mixture containing SYBR Green PCR Master Mix (Bio-Rad) and primers, and then quantitative PCR (qPCR) was performed using MyiQ Single Color Real-time PCR Detection System according to the manufacturer's protocol (Bio-Rad). All primers were designed using Primer 3. The primers were as follows, for *IREB2*: (forward) 5'-TTGTTGGAAGCTGCTGTACG-3', and (reverse) 5'-GGAAAAGGGCACTTCAACA-3'; for *LOC123688*: (forward) 5'-GGAACAAGCCTCTGCGTTAG-3', and (reverse) 5'-GGCCATCTTTGGTTTTTGA-3'; for *PSMA4*: (forward) 5'-GGAGCCAATACCTTGTGAGC-3', and (reverse) 5'-CCAGCCAATGTACAGCAATG-3'; for *CHRNA5*: (forward) 5'-GTTCTGTCCTGTGGAACACCT-3', (reverse) 5'-TTCTCATCCACATCCACCAA-3'; for *CHRNA3*: (forward) 5'-TGTCTCAGCTGGTGAAGGTG-3', and (reverse) 5'-CCATAGTCAGAGGGTTCCA-3'; for *CHRNA4*: (forward) 5'-CCCAGCTTATCAGCGTGAAT-3', (reverse) 5'-CAGGCGGTAATCAGTCCATT-3'; and for β-actin: (forward) 5'-CAAGAGATGGCCAGGGCTGCT-3', and (reverse) 5'-TCCTTCTGCATCCTGTCTGGCA-3'. All qPCR reactions were performed in triplicate.

Caspase-3/7 activity assay

Apoptosis was determined using SendoLyte™ Homogeneous Rh110 Caspase-3/7 Assay kit (ANASPEC). Cells grown in 100-mm culture dishes were washed with PBS and collected by trypsinization. An aliquot containing 1 × 10⁵ cells was precipitated and lysed in 150 μL 1× lyse buffer. Caspase-3/7 substrate solution (50 μL) was further added, and the reaction mixture was incubated at RT for 14 h. The end point fluorescence intensity was measured by

a fluorescence microplate reader at Ex/Em of 496 nm/520 nm. All apoptosis assays were performed in triplicate.

Proteasome activity assays

The assay was performed as described (16) with modifications. Briefly, cells were washed with PBS and then collected with a rubber policeman in a lysis buffer containing 50 mmol/L Tris-HCl (pH 8.0), 5 mmol/L EDTA, 150 mmol/L NaCl, 0.5% NP40, 0.5 mmol/L DTT, and a protease inhibitor cocktail (Roche). The suspended cells were incubated on ice for 15 min with occasional vortexing. Lysates were spun at top speed in a microcentrifuge at 4°C for 20 min and supernatants were collected. An aliquot containing 100 µg of lysates was incubated with 20 mmol/L fluorogenic peptide substrates Suc-LLVY-AMC and Z-LLE-AMC (Calbiochem) in 100 µL for 90 min at 37°C. The end point fluorescence intensity was measured by a fluorescence microplate reader at Ex/Em of 380 nm/460 nm. All proteasome activity analyses were performed in triplicate.

Western blotting

Eighty to 90% confluent cells in each well of six-well plates were lysed in 250 µL of 1× LDS buffer (Invitrogen) containing proteinase and phosphatase inhibitor cocktails (Sigma), sonicated, and then boiled for 10 min. Twenty microliters of each sample were resolved on SDS-PAGE and immunoblotting analyzed with the indicated antibodies. Proteins were visualized with horseradish peroxidase–conjugated secondary antibodies (Amersham Biosciences) and an enhanced chemiluminescent substrate kit (Pierce).

Haplotype analysis of 15q24-25.1 locus

Haplotype-based association analysis was performed on the 15q24-25.1 locus using 194 familial lung cases and 219 cancer-free controls from the GELCC collections (12). A total of 251 SNPs spanning from 76,016,651 to 76,992,181 bases on the 15q24-25.1 locus were analyzed. To exhaustively exploit the haplotype information, we then subjected alleles (contiguous sets of markers) from sliding windows of all sizes to haplotype association tests. Haplotype analyses were implemented in the statistical package PLINK.¹² Both omnibus/global association statistic and haplotype-specific statistic were computed. The haplotype-specific analysis tests each haplotype against all of the other haplotypes using χ^2 with one degree of freedom (df). In total, H-1 haplotype-specific tests were performed at each location in which H was the number of haplotypes at that location. The omnibus association analysis jointly estimates all haplotype effects at a location using a single χ^2 with H-1 df. At each location, the omnibus association analysis is first performed to assess the overall association. If the overall association is significant, then the haplotype-specific analysis will be performed to determine which haplotype at that location shows the strongest evidence for an association with familial lung cancer susceptibility.

Results

Fine mapping of 15q24-25.1 locus

To refine the 15q24-25.1 locus, we performed haplotype-based association analysis using 194 familial lung cases and 219 cancer-free controls from the GELCC collections (Fig. 1). To exhaustively exploit the haplotype information, we analyzed haplotypes ranging from 3 to 15 contiguous SNPs in the 15q24-25.1 locus and identified two distinct subregions that showed the most significant associations with familial lung cancer. The subregion on the left side of the 15q24-25.1 locus (named *hapL*) encompasses eight SNPs (rs16969899, rs13180,

¹²<http://pngu.mgh.harvard.edu/~purcell/plink/>

rs16969914, rs9788682, rs9788721, rs8034191, rs10519203, and rs7163730) and spans 32.4 kb. Omnibus/global association analysis yielded a P value of 2.71×10^{-6} at *hapL*. Eight haplotypes were detected with frequencies of $>1\%$ at *hapL*. Among them, the haplotype *ATAGCGCA* showed the strongest association with familial lung cancer ($P = 3.20 \times 10^{-6}$). This haplotype is a risk allele with a frequency of 38.12% in cases versus 20.54% in controls, whereas three less common haplotypes, *ATAGCGCG*, *ACAATATG*, and *ACAGTATA*, reduce the risk of lung cancer (Table 1). The subregion on the right side of the 15q24-25.1 locus (named *hapN*) encompasses 12 SNPs (rs8040868, rs8192475, rs3743072, rs17487223, rs950776, rs11072768, rs11637890, rs11072773, rs12900519, rs12594550, rs12905641, and rs11857532) and spans 57.1 kb. The haplotype *CCCGAACGCTGGC* had the strongest association with familial lung cancer at *hapN* ($P = 1.51 \times 10^{-6}$).

On the 15q24-25.1 locus, *IREB2*, *LOC123688*, and *PSMA4* are within or around *hapL*, whereas the nAChR subunit genes *CHRNA5*, *CHRNA3*, and *CHRNA4* are within or around *hapN*. It is likely that the two subregions may have distinct roles in lung cancer susceptibility. Gene(s) around *hapL* may regulate cell proliferation and/or apoptosis in the lung and thus predispose smokers to lung cancer (a direct effect), whereas gene(s) around *hapN* may affect nicotine dependence and propensity to smoke and thus increase the likelihood of developing lung cancer (an indirect effect). nAChRs have previously been implicated in nicotine dependence and related phenotypes (9–12,17–19). The present study uses gene overexpression and/or gene knockdown and apoptosis analyses to determine if any gene(s) around *hapL* mediates effects on lung cancer cell growth *in vitro*.

***IREB2*, *LOC123688*, *PSMA4*, and lung cancer cell proliferation**

To determine whether genes around the *hapL* play a role in regulating human lung cancer cell proliferation, *IREB2*, *LOC123688*, and *PSMA4* were first overexpressed in A549 and H1299 cells. For unknown reasons, we could only increase the *PSMA4* transcript levels up to 1-fold in both cell lines and the *IREB2* transcript levels up to 1-fold in A549 (Supplementary Fig. S1). Consequently, we opted to conduct gene knockdown experiments using short hairpin RNAs. Effective individual knockdown of *IREB2*, *LOC123688*, and *PSMA4* in A549 and H1299 cells was examined by RT-qPCR (Fig. 2A, a). Next, we measured cell growth by MTT cell proliferation assay and found that *LOC123688* knockdown had no effect on cell growth, whereas *PSMA4* knockdown slowed down both A549 and H1299 cell proliferation compared with vector control cells (Fig. 2A, b). *IREB2* knockdown in A549 cells slightly promoted cell growth, but had no effect on H1299 cell growth (Fig. 2A, b). We further tested to see if the growth inhibition was mediated through apoptosis and found that caspase-3/7 activity was only significantly increased in both A549 and H1299 cells when *PSMA4* was knocked down (Fig. 2A, c). *IREB2* and *LOC123688* knockdown in A549 and H1299 cells did not affect apoptotic status in these cell lines (Fig. 2A, c). We also examined the effect of *PSMA4* on nontumorigenic HBEC3KT, a human bronchial epithelial cell line. Overexpression of *PSMA4* in HBEC3KT cells increased the transcript level of *PSMA4* up to 9-fold (Fig. 2B, a), but not the rate of proliferation of HBEC3KT cells (Fig. 2B, b). Collectively, our data suggest that *PSMA4* has a role in regulating human lung cancer cell proliferation and apoptosis.

***CHRNA5*, *CHRNA3*, *CHRNA4*, and lung cancer cell proliferation**

To determine the candidacy of genes around the *hapN* and to see if they play a direct role in modulating cancer cell proliferation, *CHRNA5*, *CHRNA3*, and *CHRNA4* were overexpressed in A549 and H1299 cells. RT-qPCR analysis revealed that overexpression of *CHRNA5* in H1299 cells and overexpression of *CHRNA3* and *CHRNA4* in A549 and H1299 cells were significant, whereas overexpression of *CHRNA5* in A549 cells was less efficient (Fig. 3A). MTT cell proliferation assays showed that the overexpression of these genes did not have

significant and consistent effects on the regulation of A549 and H1299 cell growth compared with vector control cells (Fig. 3B).

As the overexpression of *CHRNA5* in A549 cells was not significant, we decided to use gene knockdown to explore the role of *CHRNA5* on A549 cell growth. Successful *CHRNA5* knockdown in A549 cells was examined by RT-qPCR (Fig. 3C). MTT cell proliferation analysis revealed that *CHRNA5* knockdown did not alter A549 cell growth compared with vector control cells (Fig. 3D). Moreover, caspase-3/7 activity analyses showed similar enzyme activity between A549 vector control cells and A549 *CHRNA5* knockdown cells, indicating that these cells had similar apoptotic statuses (Fig. 3E).

Taken together, our data show that altering the expression levels of *CHRNA5*, *CHRNA3*, and *CHRNA4* do not affect A549 and H1299 cell proliferation, suggesting that these genes are not required to maintain cancer cell proliferation.

PSMA4-dependent proteasome activity

The 26S proteasome is a biological macromolecule consisting of a variety of structural and catalytic subunits. The 26S proteasome functions as multicatalytic proteinases containing chymotrypsin-like (CT-like) and peptidylglutamyl peptide hydrolyzing-like (PGPH-like) proteolytic activities. Altering the stoichiometry of the PSMA4 structural subunit with other proteasomal subunits may affect proteasomal proteolytic activities. We followed proteasomal CT- and PGPH-like proteolytic activities and examined the effect of *PSMA4* knockdown on proteasome activities in A549 *PSMA4* knockdown versus A549 vector control cells. Knocking down *PSMA4* reduced proteasomal CT- and PGPH-like activities to 50% of that observed in vector control activities (Fig. 4A). This result showed that PSMA4 is required for maintaining normal proteasomal catalytic activities. A consequence of the decreased proteasome activity was an increase in the number of ubiquitinated proteins in A549 *PSMA4* knockdown cells compared with A549 control cells (Fig. 4B).

Increased *PSMA4* transcripts in human lung cancers

Although *in vitro* overexpression of *PSMA4* yielded almost no increase in transcription levels, gene knockdown analysis, in turn, confirmed that *PSMA4* plays a role in modulating cell proliferation. To see if the expression of *PSMA4* is altered in human NSCLC, the abundance of *PSMA4* transcripts in 52 paired human normal lung and lung tumor samples was examined by RT-qPCR. Of the 52 paired samples, 21 (40.4%) had increased levels (>1.5-fold) of *PSMA4* transcripts in the tumor, 1 (1.9%) had decreased levels (<0.5-fold), and 30 (57.7%) had no change (0.5–to 1.5-fold; Fig. 5). These 52 paired samples include acinar adenocarcinoma, bronchioloalveolar adenocarcinoma, adenocarcinoma NOS, papillary adenocarcinoma, adenosquamous carcinoma, epidermoid squamous cell carcinoma, keratinizing squamous cell carcinoma, and squamous cell carcinoma NOS. The percentage of paired samples with increased *PSMA4* transcripts in the tumors varied from 30% to 60% among different histologic types of lung cancer, except for papillary adenocarcinoma that only had a 20% increase (Fig. 5). As shown in Fig. 5, cell type seems important in terms of *PSMA4* overexpression. However, except for one tumor sample from the subtype adenosquamous carcinoma showing decreased expression of PSMA4, all other samples from the different subtypes showed either no changes or increased expression in *PSMA4*. Thus, although *PSMA4* expression varied considerably among different lung cancer subtypes, in general, tumor samples from these different lung subtypes tend to show increased expression of *PSMA4* compared with their pair-matched normal tissues. This result indicates that, *in vivo*, expression of *PSMA4* is up-regulated in almost half of all lung cancers.

Discussion

Recent efforts to elucidate genetic factors in lung cancer susceptibility have identified the chromosome 15q24-25.1 locus (9–11). The 15q24-25.1 locus contains an iron metabolism protein gene *IREB2*, a 20S proteasome structural protein gene *PSMA4*, three nAChR subunit genes *CHRNA5*, *CHRNA3*, and *CHRNA4*, and a hypothetical gene *LOC123688*. An ongoing question is which among the six candidates accounts for an increased risk of lung cancer. In the current study, we have fine-mapped the 15q24-25.1 locus into two subregions: *hapL* for *IREB2*, *LOC123688*, and *PSMA4*; and *hapN* for *CHRNA5*, *CHRNA3*, and *CHRNA4*. Our *in vitro* investigation into the genes around *hapL* as modulators of tumor cell proliferation implicated *PSMA4* as a strong candidate. This result is physiologically relevant for two reasons. First, there is endogenous expression of *PSMA4* in the two human cancer cell lines used in this study, and second, expression of *PSMA4* is upregulated in lung cancer as well as in other cancer types.

At present, there is no evidence that SNP status of these genes is directly linked to the mitogenic activity of their protein products. Haplotype or SNP data neither reflect genetic changes (such as at the mRNA/protein expression level or protein function) of the candidate gene(s) in detail, nor tell whether these genetic changes could alter biological functions. Identifying causal genetic variants in the candidate gene(s) is very challenging and requires further extensive genetic and biological investigations. Any genetic change will eventually be exhibited at the mRNA/protein level or protein function to play biological function. Therefore, *in vitro* changing gene expression levels via overexpression/knockdowns and assaying for proliferation and apoptosis would be more efficient and informative. By these approaches, we have shown that *PSMA4* affects lung cancer cell proliferation and apoptosis. This result suggests that *PSMA4* is a candidate lung cancer susceptibility gene in the 15q24-25.1 locus, although the other five candidate genes in this high linkage disequilibrium region cannot be completely excluded. Our *in vitro* analyses were limited to human lung cancer (lung cancer cell lines and lung cancer samples). However, the role of *PSMA4* in leading tumorigenesis may not be limited to lung cancer. Similar to other oncogene/tumor suppressor genes, such as *P53* and *PTEN*, elevated expression of *PSMA4* is also found in other human cancer types.

The 26S proteasome contains one 20S proteasome core and two 19S regulatory caps. The 20S proteasome core is hollow and forms an enclosed cavity where proteins are degraded. The 20S proteasome core contains two types of subunits: α subunits are structural and serve as docking domains for proteasome assembly and regulators of proper function; β subunits are predominantly catalytic (14). *PSMA4*, a proteasome α type subunit 4, has been characterized as a structural subunit of the 20S proteasome core (14,15). Our preliminary biological analysis revealed that *PSMA4* governs proteasome activity. We showed *in vitro* that knockdown of *PSMA4* expression decreases proteasome activity and results in the accumulation of ubiquitinated proteins. This proteasome is responsible for the degradation of proteins involved in the activation or repression of many cellular processes, including transcription, cell-cycle progression, and apoptosis. Therefore, proteasome dysfunction stresses cells. In our case, knockdown of *PSMA4* expression in cancer cells induced apoptosis. Cancer cells show increased proliferation and decreased apoptosis *in vivo* via various mechanisms. Our findings that the down-regulation of *PSMA4* expression induces apoptosis and that *PSMA4* expression is increased in nearly half of the lung cancers studied suggest that upregulation of proteasome activity may be a novel mechanism of tumorigenesis. Indeed, inhibition or down-regulation of proteasome activity by proteasome inhibitors has already been adopted as a form of cancer treatment (20). Therefore, our findings strongly suggest that *PSMA4* plays a direct role in cancer cell proliferation.

We also systemically evaluated the nAChR subunit genes, particularly *CHRNA5*, to determine if any of them has a regulatory effect on lung cancer cell growth. Recent studies have linked rs16969968, a missense SNP (D398N) in *CHRNA5*, to smoking, nicotine addiction, and lung cancer (12,21). We overexpressed *CHRNA5*-D398 in parallel with *CHRNA5*-N398 (rs16969968) in A549 and H1299 cells and did not observe any difference in growth (data not shown). Collectively, our current biological analysis of the nAChR subunit genes around *hapN* did not reveal any growth or apoptotic differences between normal lung and lung cancer cells. Our data strongly suggest that these nAChR subunit genes are not directly involved in lung cancer, but may instead affect nicotine dependence and propensity to smoke and thus indirectly increase the likelihood of developing lung cancer.

In summary, we have shown for the first time that *PSMA4* at the 15q24-25.1 locus plays a direct role in regulating lung cancer cell growth. Further understanding of the molecular mechanisms of the candidate genes may result in the development of new strategies for prevention, early detection, diagnosis, and treatment of lung cancer and other human cancers.

Supplementary Material

Refer to Web version on PubMed Central for supplementary material.

Acknowledgments

Grant support: NIH grants U01CA76293 (Genetic Epidemiology of Lung Cancer Consortium), R01CA058554, R01CA093643, R01CA099147, R01CA099187, R01ES012063, R01ES013340, R03CA77118, R01CA80127, P30ES06096, P50CA70907 (Specialized Program of Research Excellence), N01HG65404, N01-PC35145, P30CA22453, R01CA63700, DE-FGB-95ER62060, Mayo Clinic intramural research funds, and Department of Defense VITAL grant. This study was also supported in part by NIH, the Intramural Research Programs of the National Cancer Institute, and the National Human Genome Research Institute.

We thank the Fernald Medical Monitoring Program (FMMP) for sharing their biospecimens and data with us. We thank Dr. Jay W. Tichelaar and Dr. Haris G. Vikis for their critical comments on the manuscript, and Tiffany Wu and Kristen Baker for their English proofreading of the manuscript.

References

1. Jemal A, Siegel R, Ward E, et al. Cancer statistics, 2008. *CA Cancer J Clin* 2008;58:71–96. [PubMed: 18287387]
2. Dubey S, Powell CA. Update in lung cancer 2007. *Am J Respir Crit Care Med* 2008;177:941–946. [PubMed: 18434333]
3. Hecht SS. DNA adduct formation from tobacco-specific N-nitrosamines. *Mutat Res* 1999;424:127–142. [PubMed: 10064856]
4. Mossman BT, Lounsbury KM, Reddy SP. Oxidants and signaling by mitogen-activated protein kinases in lung epithelium. *Am J Respir Cell Mol Biol* 2006;34:666–669. [PubMed: 16484683]
5. Heeschen C, Jang JJ, Weis M, et al. Nicotine stimulates angiogenesis and promotes tumor growth and atherosclerosis. *Nat Med* 2001;7:833–839. [PubMed: 11433349]
6. Heeschen C, Weis M, Aicher A, Dimmeler S, Cooke JP. A novel angiogenic pathway mediated by non-neuronal nicotinic acetylcholine receptors. *J Clin Invest* 2002;110:527–536. [PubMed: 12189247]
7. Heeschen C, Weis M, Cooke JP. Nicotine promotes arteriogenesis. *J Am Coll Cardiol* 2003;41:489–496. [PubMed: 12575981]
8. Lindstrom J. Nicotinic acetylcholine receptors in health and disease. *Mol Neurobiol* 1997;15:193–222. [PubMed: 9396010]

9. Thorgeirsson TE, Geller F, Sulem P, et al. A variant associated with nicotine dependence, lung cancer and peripheral arterial disease. *Nature* 2008;452:638–642. [PubMed: 18385739]
10. Amos CI, Wu X, Broderick P, et al. Genome-wide association scan of tag SNPs identifies a susceptibility locus for lung cancer at 15q25.1. *Nat Genet* 2008;40:616–622. [PubMed: 18385676]
11. Hung RJ, McKay JD, Gaborieau V, et al. A susceptibility locus for lung cancer maps to nicotinic acetylcholine receptor subunit genes on 15q25. *Nature* 2008;452:633–637. [PubMed: 18385738]
12. Liu P, Vikis HG, Wang D, et al. Familial aggregation of common sequence variants on 15q24-25.1 in lung cancer. *J Natl Cancer Inst* 2008;100:1326–1330. [PubMed: 18780872]
13. LaVaute T, Smith S, Cooperman S, et al. Targeted deletion of the gene encoding iron regulatory protein-2 causes misregulation of iron metabolism and neurodegenerative disease in mice. *Nat Genet* 2001;27:209–214. [PubMed: 11175792]
14. Nandi D, Woodward E, Ginsburg DB, Monaco JJ. Intermediates in the formation of mouse 20S proteasomes: implications for the assembly of precursor β subunits. *EMBO J* 1997;16:5363–5375. [PubMed: 9311996]
15. Davoli R, Fontanesi L, Russo V, et al. The porcine proteasome subunit A4 (PSMA4) gene: isolation of a partial cDNA, linkage and physical mapping. *Anim Genet* 1998;29:385–388. [PubMed: 9800328]
16. Eguchi H, Herschenhou N, Kuzushita N, Moss SF. *Helicobacter pylori* increases proteasome-mediated degradation of p27(kip1) in gastric epithelial cells. *Cancer Res* 2003;63:4739–4746. [PubMed: 12907657]
17. Berrettini W, Yuan X, Tozzi F, et al. α -5/ α -3 nicotinic receptor subunit alleles increase risk for heavy smoking. *Mol Psychiatry* 2008;13:368–373. [PubMed: 18227835]
18. Bierut LJ, Stitzel JA, Wang JC, et al. Variants in nicotinic receptors and risk for nicotine dependence. *Am J Psychiatry* 2008;165:1163–1171. [PubMed: 18519524]
19. Stevens VL, Bierut LJ, Talbot JT, et al. Nicotinic receptor gene variants influence susceptibility to heavy smoking. *Cancer Epidemiol Biomarkers Prev* 2008;17:3517–3525. [PubMed: 19029397]
20. McConkey DJ, Zhu K. Mechanisms of proteasome inhibitor action and resistance in cancer. *Drug Resist Updat* 2008;11:164–179. [PubMed: 18818117]
21. Saccone SF, Hinrichs AL, Saccone NL, et al. Cholinergic nicotinic receptor genes implicated in a nicotine dependence association study targeting 348 candidate genes with 3713 SNPs. *Hum Mol Genet* 2007;16:36–49. [PubMed: 17135278]

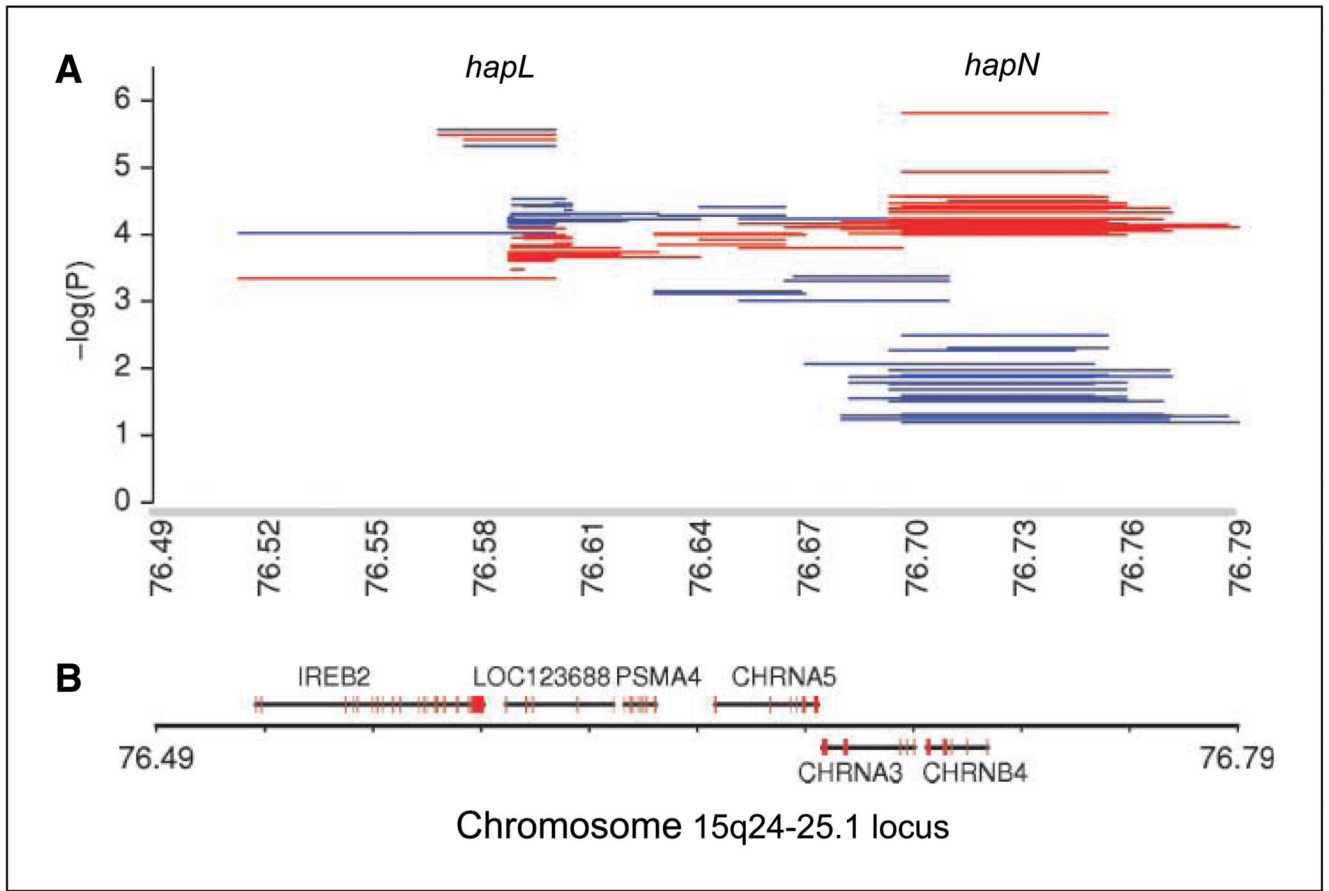
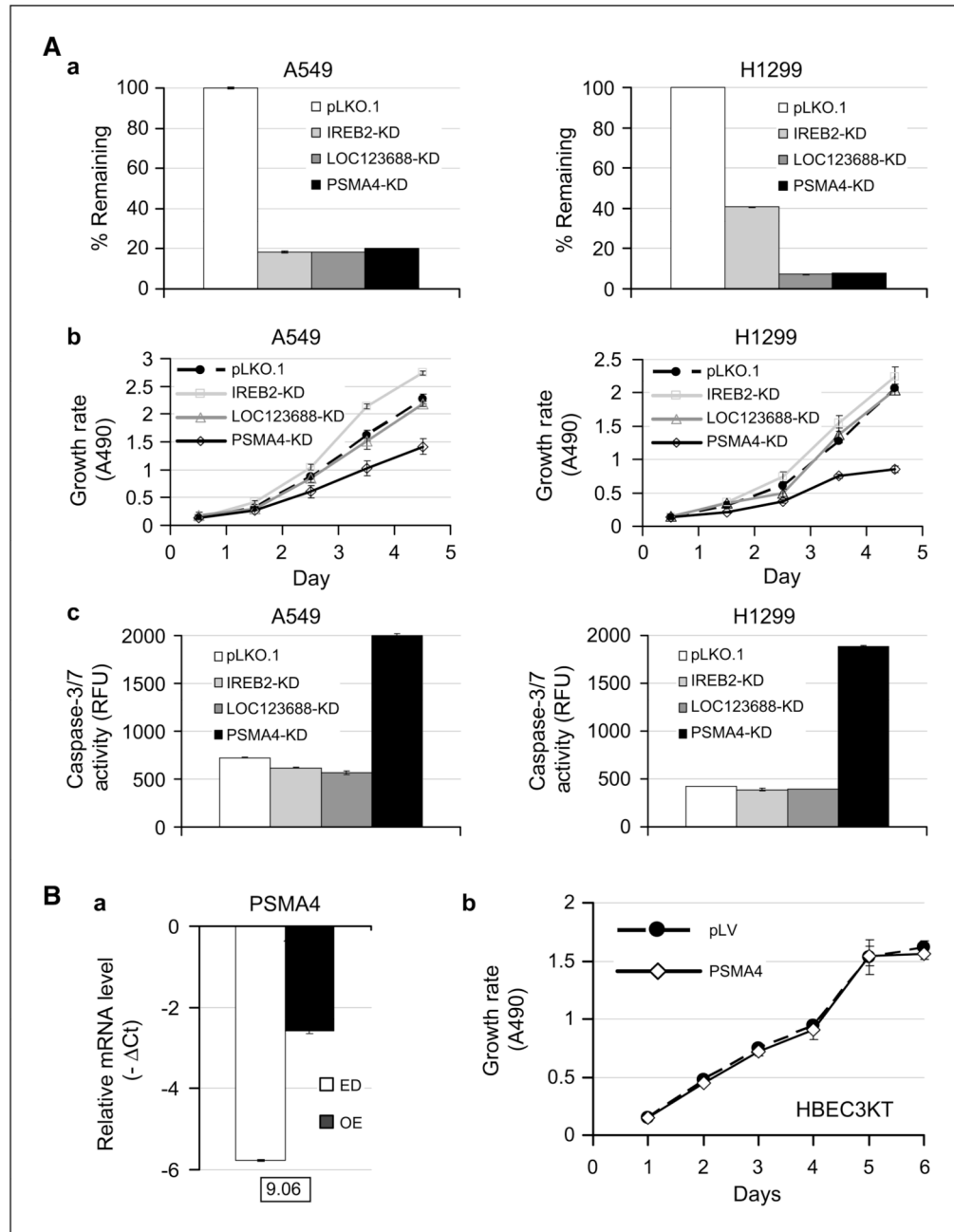


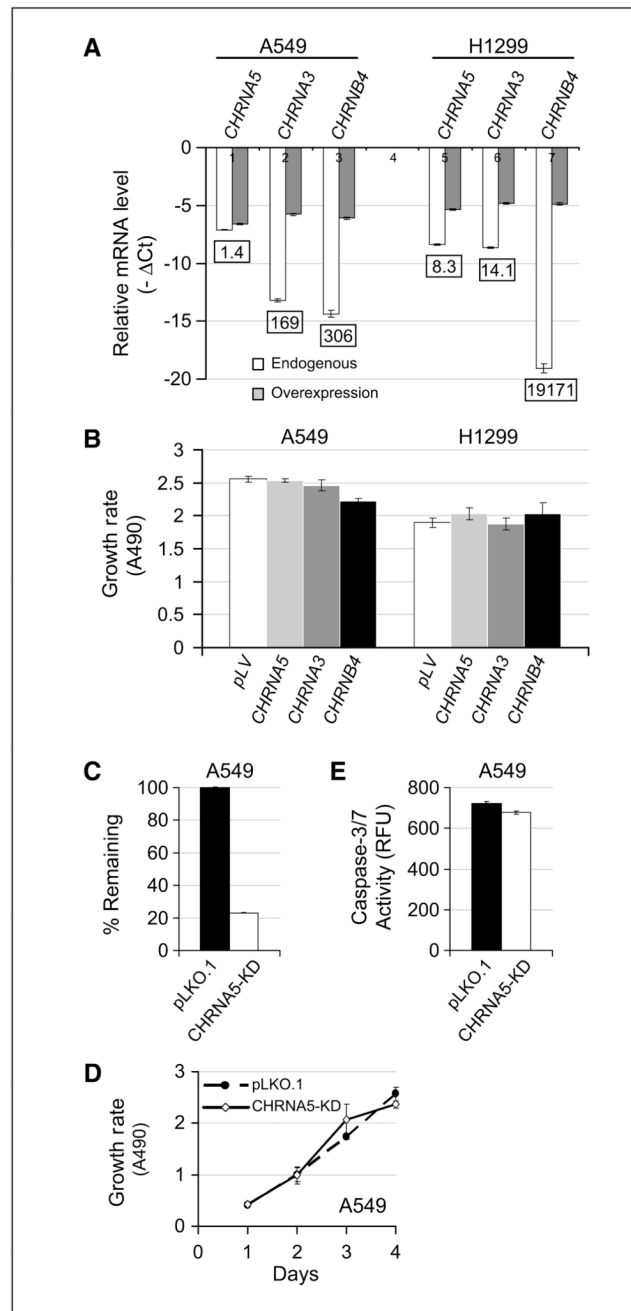
Figure 1.

Haplotype analysis of the 15q24-25.1 locus. *A*, association of haplotypes with familial lung cancer susceptibility in the GELCC collections. *Blue lines*, the results from omnibus/global haplotype analysis; *red lines*, the results from individual haplotype analysis. *B*, physical map of the 15q24-25.1 locus.

**Figure 2.**

Effects of *IREB2*, *LOC123688*, and *PSMA4* on A549 and H1299 human lung cancer cell growth and apoptosis. **A**, effects of *IREB2*, *LOC123688*, and *PSMA4* knockdown on A549 and H1299 human lung cancer cell growth and apoptosis. **a**, results of *IREB2*, *LOC123688*, and *PSMA4* knockdown by RT-qPCR analyses. *Columns*, mean percentage of the target gene remaining; *bars*, SD of the mean in at least three individual experiments. **b**, growth curves of *IREB2*, *LOC123688*, and *PSMA4* knockdown versus empty vector knockdown by MTT assay. **c**, results of caspase-3/7 activity assays with and without *IREB2*, *LOC123688*, and *PSMA4* expression. *Columns*, mean relative fluorescence unit (RFU). A larger RFU value represents a higher caspase-3/7 activity and thus a stronger apoptotic response.

PSMA4 knockdown in lung cancer cells inhibited cell growth and induced apoptosis. *KD*, knockdown. *B*, effects of *PSMA4* overexpression on HBEC3KT nontumorigenic human bronchial epithelial cell growth. *a*, results of *PSMA4* overexpression versus endogenous expression in HBEC3KT cells by RT-qPCR analysis. *Columns*, mean $-\Delta\text{Ct}$ values (threshold cycle of β -actin minus threshold cycle for target gene). A larger $-\Delta\text{Ct}$ value represents a higher abundance of the transcript. The numbers in the boxes are the fold increase after overexpression. *ED*, endogenous; *OE*, overexpression. *b*, growth curves of *PSMA4* overexpression versus empty vector overexpression by MTT assay. All assays were performed in triplicate.

**Figure 3.**

CHRNA5, *CHRNA3*, *CHRNB4*, and human lung cancer cell proliferation. **A**, results of *CHRNA5*, *CHRNA3*, and *CHRNB4* overexpression versus endogenous expression in A549 and H1299 cells by RT-qPCR analysis. *Columns*, mean $-\Delta\text{Ct}$ values. The numbers in the boxes are the fold increase after overexpression. **B**, effects of *CHRNA5*, *CHRNA3*, and *CHRNB4* overexpression on A549 and H1299 cell growth by MTT proliferation assays. One thousand cells per well in 100 μL were seeded into 96-well plates for 12 h, and then viable cells were measured by MTT analysis (see text for details) on daily pace for up to 4 d for A549 and 6 d for H1299 cells. *Columns*, mean MTT values (A490). **C**, results of *CHRNA5* knockdown by RT-qPCR analyses. *Columns*, mean percentage of the target gene remaining.

D, growth curves of *CHRNA5* knockdown versus empty vector knockdown by MTT assay. *E*, results of caspase-3/7 activity assays with and without *CHRNA5* expression. *Columns*, mean RFU. *KD*, knockdown.

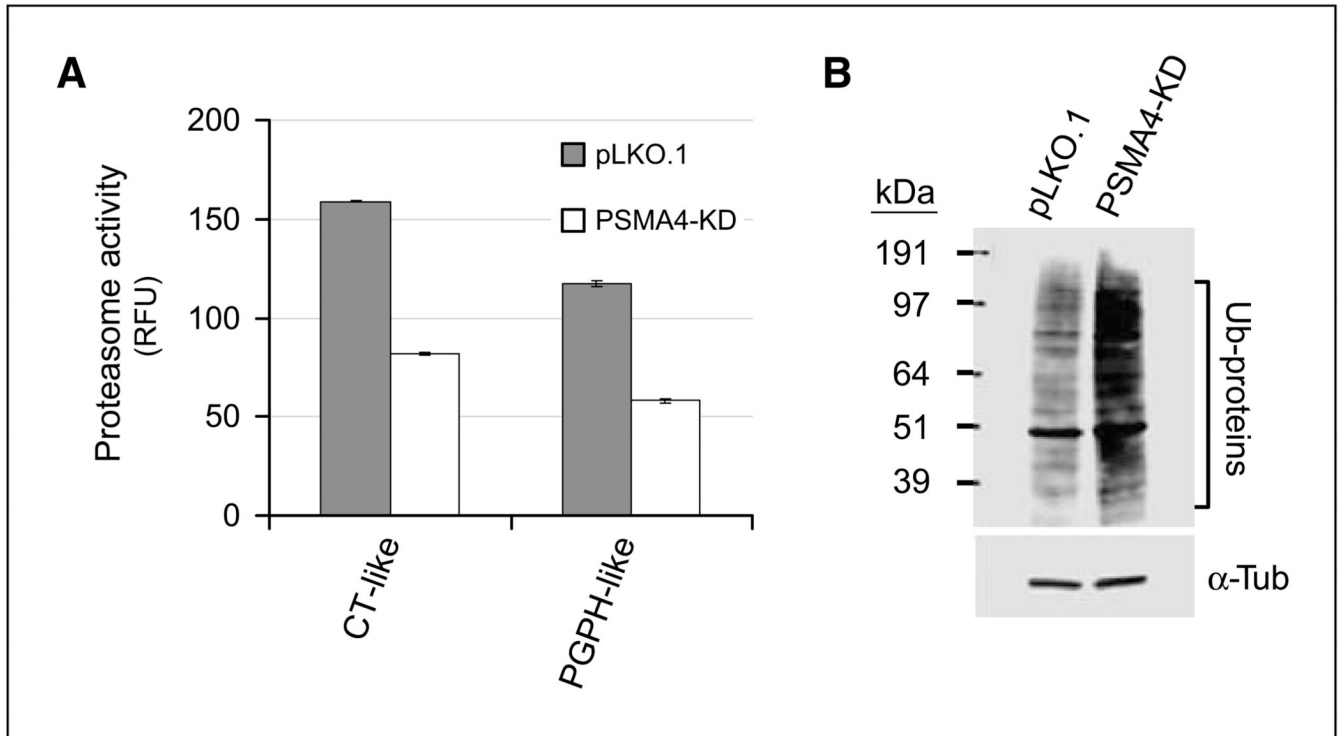


Figure 4. *PSMA4*-dependent proteasome activity. *A*, effects of *PSMA4* knockdown on 26S proteasome activity. Proteasomal CT- and PGPH-like activities were measured. *Columns*, mean proteasomal CT- or PGPH-like activities (RFU). *B*, the lysates used in Fig. 4A were resolved on SDS-PAGE and analyzed by immunoblotting with the indicated antibodies. *KD*, knockdown.

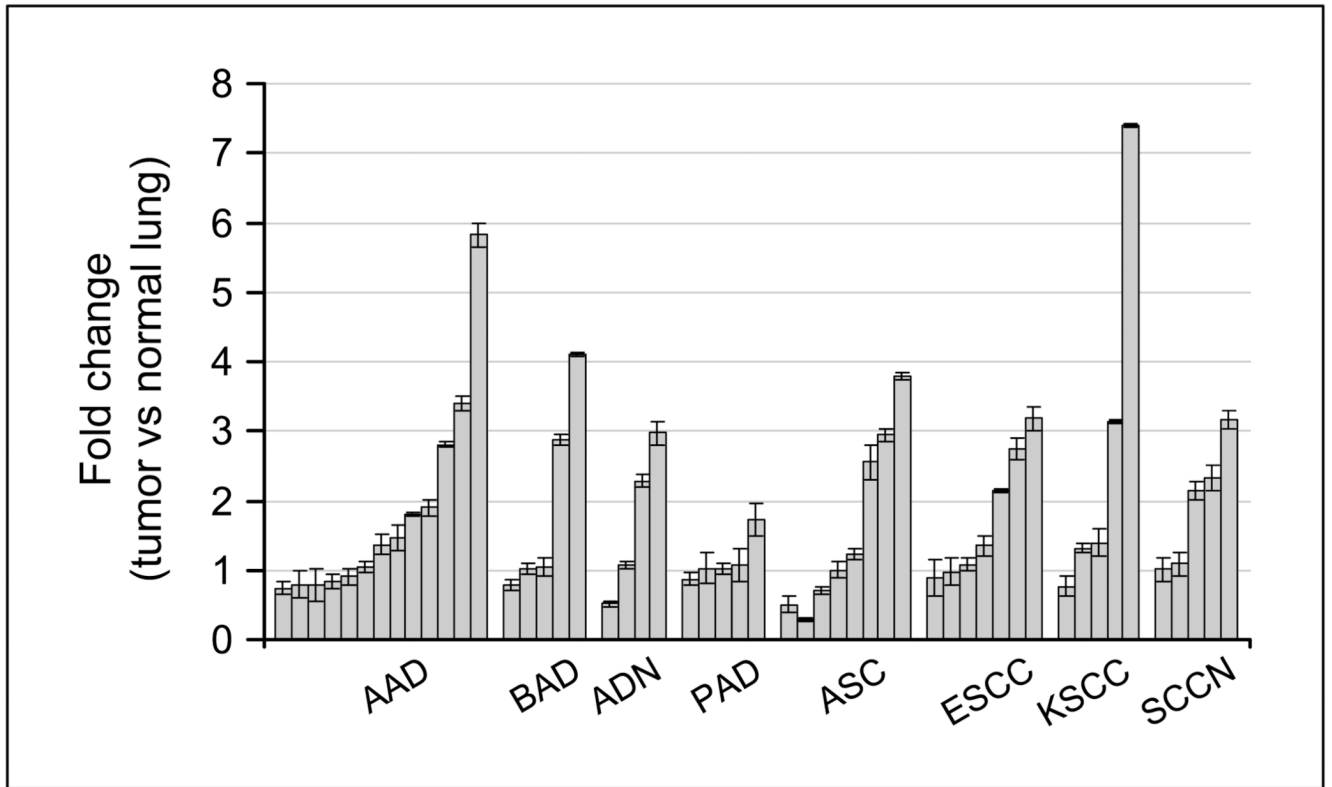


Figure 5.

RT-qPCR analysis of *PSMA4* transcript levels using total RNA samples from 52 paired tumor and normal tissues of the lung. *Columns*, mean values of fold change in *PSMA4* expression in lung tumor versus normal lung tissues of the same patient. *ADD*, acinar adenocarcinoma; *BAD*, bronchioloalveolar adenocarcinoma; *ADN*, adenocarcinoma NOS; *PAD*, papillary adenocarcinoma; *ASC*, adenosquamous carcinoma; *ESCC*, epidermoid squamous cell carcinoma; *KSCC*, keratinizing squamous cell carcinoma; and *SCCN*, squamous cell carcinoma NOS. All RT-qPCRs were performed in triplicate. *PSMA4* transcript level was increased in 40% of human NSCLCs.

Table 1

Two haplotypes are associated with familial lung cancer

Haplotypes	Frequency		<i>P</i>
	Cases	Controls	
<i>HapL</i>			
<i>OMNIBUS</i>	NA	NA	2.71×10^{-6}
<i>ACAATATA</i>	0.0339	0.0659	0.083
<i>ATAGCGCG</i>	0.0344	0.0832	0.014
<i>ACAATATG</i>	0.1101	0.1928	0.006
<i>ATAGCGCA</i>	0.3812	0.2054	3.20×10^{-6}
<i>ATAGTATA</i>	0.2514	0.2525	0.976
<i>CCAGTATA</i>	0.1707	0.1687	0.949
<i>ACAGTATA</i>	0.0009	0.0259	0.012
<i>CCAGCGCA</i>	0.0174	0.0056	0.177
<i>HapN</i>			
<i>OMNIBUS</i>	NA	NA	0.003
<i>TTCGAACGCTGGC</i>	0.0129	0.0194	0.564
<i>TTCGGACGCTGGC</i>	0.0303	0.0547	0.179
<i>CCCGAACGCTGGA</i>	0.0100	0.0310	0.103
<i>CCCGAACGCTGGC</i>	0.3934	0.2002	1.51×10^{-6}
<i>CCCGAACGCCGGA</i>	0.0399	0.0559	0.403
<i>TTCGGAAGCTGAA</i>	0.0113	0.0207	0.408
<i>TTCGGAAGCTCGC</i>	0.0638	0.1073	0.084
<i>TTCGGGCCCTGAA</i>	0.2884	0.3008	0.759
<i>TTCGGGCCCTGGC</i>	0.0316	0.0294	0.889
<i>TTCGGGCCCCGGA</i>	0.0183	0.0251	0.603
<i>TTCGGAAGCTCGA</i>	0.0478	0.0883	0.074
<i>TTCGGACCCTGAA</i>	0.0045	0.0211	0.107
<i>TTCGGGCGCTGGC</i>	0.0132	0.0142	0.918
<i>CCTGGACCCTGGC</i>	0.0347	0.0319	0.857

NOTE: *HapL* spans 76,569,381 to 76,601,736 bp, and consists of rs16969899, rs13180, rs16969914, rs9788682, rs9788721, rs8034191, rs10519203, and rs7163730. *HapN* spans 76,698,236 to 76,755,323 bp, and consists of rs8040868, rs8192475, rs3743072, rs17487223, rs950776, rs11072768, rs11637890, rs11072773, rs12900519, rs12594550, rs12905641, and rs11857532.

Abbreviation: NA, not applicable.